Hindawi Publishing Corporation
Journal of Quantum Chemistry
Volume 2014, Article ID 149380, 8 pages
http://dx.doi.org/10.1155/2014/149380

Research Article

Quantum Chemical Study of Mixed-Ligand Monometallic Ruthenium(II) Complex of Composition $[(bpy)_2Ru(H_3Imbzim)](ClO_4)_2 \cdot 2H_2O$

Mohsin Yousuf Lone and Prakash Chandra Jha

School of Chemical Sciences, Central University of Gujarat, Sector 30, Gandhinagar, Gujarat 382030, India

Correspondence should be addressed to Prakash Chandra Jha; prakash.jha@cug.ac.in

Received 29 November 2013; Revised 24 February 2014; Accepted 11 March 2014; Published 19 May 2014

Academic Editor: Yinghong Sheng

On the basis of density functional theoretical approach, we have assessed the ground state geometries and absorption spectra of recently synthesized monometallic ruthenium (II) complex of composition $[(bpy)_2Ru(H_3Imbzim)](ClO_4)_2 \cdot 2H_2O$ where bpy = 2,2′-bypyridine and H_3Imbzim = 4,5-bis(benzimidazol-2-yl)imidazole. The all different kinds of charge transfers such as ligand-ligand, and metal-ligand have been quantified, compared, and contrasted with the experimental results. In addition, the effect of solvent on excitation energies has been evaluated. In spite of some digital discrepancies in calculated and observed geometries, as well as in absorption spectra, the density functional theory (DFT) seems to explain the main features of this complex.

1. Introduction

In recent times, the importance of inorganic complexes has been reported extensively keeping in mind the wide range of applicability these complexes possess in different domains of life. Thanks to the synthetic chemists for synthesizing, characterizing, and demonstrating the wide range of applicability of these complexes. Among the entire applicability domain, the recognition and sensing of anions is one of the recently emerged and challenging areas in the field of research. This is due to the important role played by anions in the field of biological, industrial, agricultural, and environmental processes [1–8]. This importance can be visualized from the facts that majority of enzymes bind anions as either substrate or cofactor and many act as ubiquitous nucleophiles, bases, redox agents, and phase transfer catalysts [9, 10]. Diseases like cystic fibrosis and Alzheimer's are induced by the malfunction of natural anion regulation processes [11, 12]. Even, from environmental point of view, the eutrophication of water is an important issue which is caused by phosphate and nitrate ions and used in agriculture fertilizers [13–16]. The advantage of the transition metal complex of composition $[(bpy)_2Ru(H_3Imbzim)]^{2+}$ where bpy = 2,2′-bypyridine and H_3Imbzim = 4,5-bis(benzimidazol-2-yl)imidazole to act as a sensor is that it contains three potent NH bonds that can be donated for the hydrogen bonding to the anions. Given this importance, it is not surprising that extensive experimental studies have been dedicated to design of simple artificial anion receptors and sensors [17–20]. However, there is not very clear understanding about the guiding principles about the selection of right kind of moiety as a chromophore and ligand as an anion sensor. In such situation, quantum chemical based electronic structure calculations can be expected to provide us valuable information about its structural features which in turn could be further used for better understanding of structural features and hence for enhanced appreciative of the factors responsible for such properties. Recently, Debasish et al. [21] have synthesized and characterized monometallic ruthenium (II) complex of composition $[(bpy)_2Ru(H_3Imbzim)](ClO_4)_2 \cdot 2H_2O$ using standard analytical and spectroscopic techniques. On the basis of their study, they have proposed molecular structure from single crystal X-ray measurements. Furthermore, they have experimentally explored in detail the electronic absorption and emission behavior in different solvents. In this work, our aim is to complement experimental work

with quantum chemical calculations in order to have better understanding of it in the one hand while developing it with some confidence for better predicting power of some experimentally unexplored properties on the other hand. The advancement in DFT as computational methodology has reached a point where predicted properties can be expected to be of reasonable chemical accuracy.

The present paper reports the comparison between gas phase optimized geometry with X-ray geometry and determination of position of hydrogen atoms involved in hydrogen bonding, which is not possible by single crystal XRD due to its low electron density. Furthermore the assignment of gas phase electronic spectra using TD-DFT calculations and the effect of solvents on excitation energies has been carried out.

2. Methods of Calculations

All the theoretical calculations were performed with the Gaussian-03 program package [22]. Full geometry optimization in gas and solvent phase were carried out using B3LYP functional and 6-31G** [23] as basis set except for ruthenium for which we used LANL2DZ [24] pseudopotential. The hessian matrix has been calculated to make sure that the given structure is at its minima. Thereafter, the absorption spectra have been calculated as vertical electronic excitations from the ground state using TD-DFT approach with PBE1 as functional of the choice and 6-31G** basis set for all the elements present in the complex except for ruthenium for which LANL2DZ [24] has been employed as implemented in Gaussian-03 [22]. The choice of PBE1 hybrid functional [25–27] has been made as its efficiency on a wide range of compounds has been shown in the many earlier reports in literature [28]. The effect of solvent on absorption spectra was taken care by using polarizable continuum model (PCM) of Tomasi and coworkers [29]. Default parameters were used for the solvents dimethyl sulfoxide (DMSO) and acetonitrile (CH_3CN).

3. Results and Discussion

It is important to compare and contrast the essential structural parameters obtained as a result of geometry optimization with respect to experimentally reported X-ray structure [21]. The optimized geometry and the corresponding figure with numbering scheme for the title complex have been depicted in Figure 1.

The experimental data for this complex is available, results for related molecule in terms of structural parameters (bond lengths and bond angles) are included in Tables 1(a) and 1(b) for comparison, and different conclusions may be drawn by analyzing the data. It is clear from crystal structure that the monometallic complex consists of hexa-coordinated Ru^{II} center in which the Ru^{II} $(bpy)_2$ unit is coordinated to one of the two imidazole (central) nitrogen N8 and one benzimidazole nitrogen N1 of 4,5-bis(benzimidazol-2-yl)imidazole. In this complex, three different types of metal-nitrogen distances are observed. The longest Ru–N distance that involves the benzimidazole nitrogen atom is 2.093 Å. The next longest Ru–N distance, pertaining to the central imidazole nitrogen atom, is 2.077 Å. The bipyridine ligand provides shortest Ru–N distances with average value of 2.033 Å.

However, computationally calculated longest Ru–N distance involves the central imidazole nitrogen with the value equal to 2.112 Å. The next longest Ru–N distance involves the benzimidazole nitrogen atom with the value equal to 2.110 Å. The bipyridine ligand provides the shortest Ru–N distance with average value of 2.060 Å. The deviation of metal complex from the idealized octahedral geometry is reflected in their bond angles. The *cis*-angle varies from 78.42° to 79.21°, while the trans-angles vary between 170.99° and 175.35°. However, it is also reflected from the computed bond angles that this complex deviates from the regular octahedral geometry. It could be due to electronic repulsions as well as due to steric hindrances amongst the ligands. Both experimental and theoretical methods are in agreement with their observations and predictions. To be more precise, the largest deviations in bond lengths and bond angles are 0.033 Å and 2.15°, respectively. These results reflect how much theoretical methods of calculation are in agreement with the experimental methods. The comparison of different bond angles for the title complex is summarized in Table 1(b).

In monometallic Ru^{II} complex it has been experimentally found that the NH proton of metal coordinated benzimidazole side is involved in an intramolecular hydrogen bonding interaction with nitrogen atom of the free benzimidazole moiety with N–H···N distance of 2.096 Å. However, theoretically calculated N–H···N distance is 1.864 Å and N–H distance is 1.0313 Å. In addition, the complex also possesses a pair of externally directed NH protons of $H_3Imbzim^-$ which adopt *cis*-arrangement and could be used for the formation of adduct with anion via hydrogen-bonding interactions. The N–H and N–H···N distances of both the protons have not been explored experimentally because of the low electron density at hydrogen atom. However, theoretically calculated N–H and N–H···N distances of both the protons are 1.030 Å and 1.8475 Å, respectively. Since the predicted parameters for this complex are in good agreement with experimental data, thereby providing strong support for the use of these theoretical methods for structural and spectroscopic studies.

The experimentally determined electronic spectra of the Ru (II) complex exhibit a number of absorption bands in the UV-visible region. The two most intense bands are observed at around 242 and 290 nm due to π-π^* transition of bpy, while the next higher wavelength absorption occurring between 340 and 370 nm is due to ligand centered transitions of bridging ligand. In addition to these transitions, this complex exhibits two fairly intense absorptions at 475 and 425 nm and the next higher energy bands are due to Ru (dπ)-to-bpy(π^*) charge-transfer (MLCT) transitions.

The interpretation and assignment of the theoretically calculated spectra of this complex have been done on the basis of shapes of Kohn-Sham orbitals. All types of charge transfers have been found in this complex, these include ligand centered transfer of bridged ligands towards the central metal atom (LMCT) or between the ligands (LL), and sometimes it

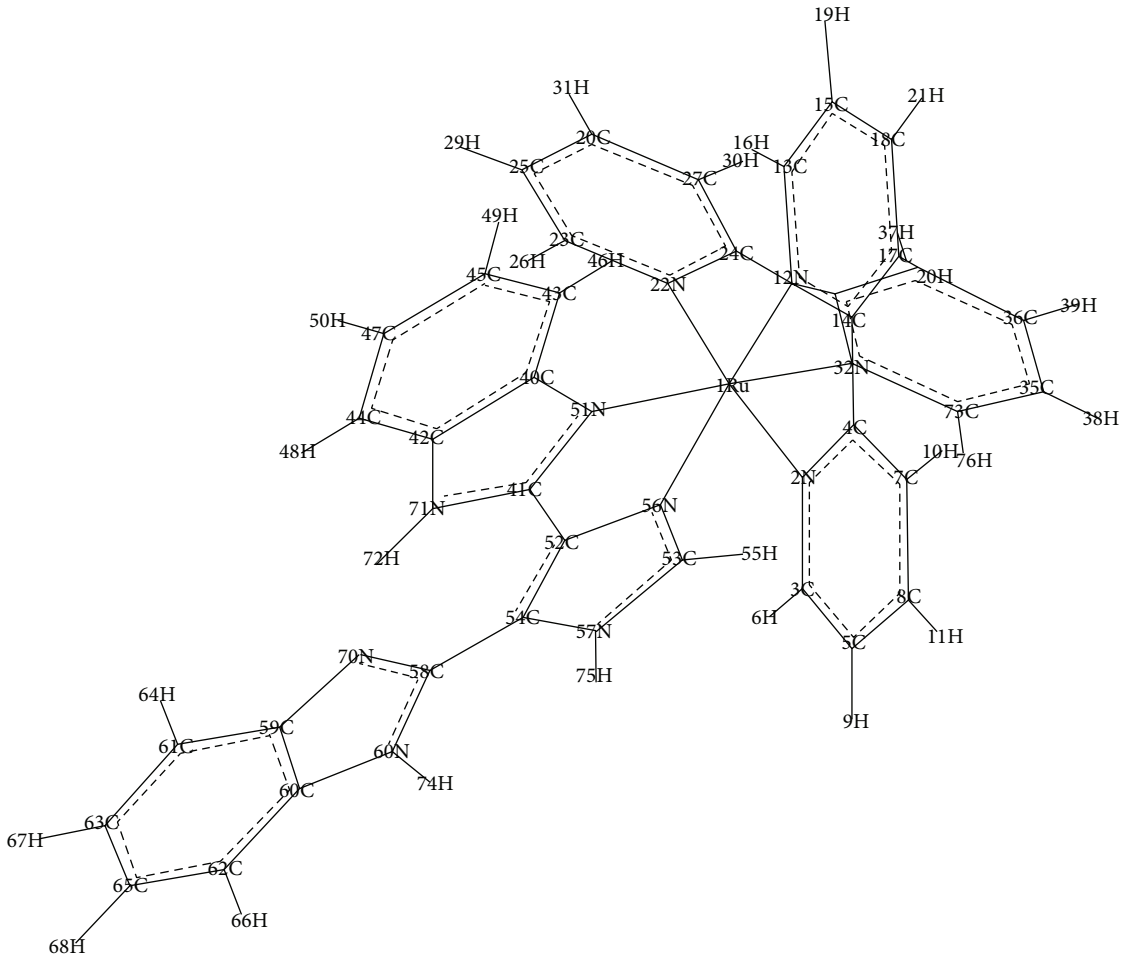

Figure 1: Numbering scheme of the complex molecule.

has been found that the charge transfer occurs from the central metal atom to the ligands (MLCT). In addition to these charge transfers, the complex also displays *d-d* transitions. Even though, theoretically, it is possible to explain nature of each and every transition, but here we will try to compare the transitions of prime interest. The intense bands due to π-π^* transitions of ligands are observed at 235 and 286 nm. These transitions can be depicted from the transference of electron density from the molecular orbitals 159 → 171, 159 → 172, 160 → 171, 161 → 172, 161 → 173, 161 → 174, 162 → 173, 162 → 174, 163 → 173, 163 → 174 and 161 → 170, 162 → 168, 162 → 169, 162 → 170, 165 → 172, 165 → 173, 166 → 173, and 167 → 175, respectively. The transitions occurring between 377 and 360 nm are due to ligand centered transitions of the bridging ligand which can be depicted from the transitions taking place from the molecular orbitals 163 → 170, 164 → 170, 165 → 170, 166 → 170, and 167 → 170. In addition to these transitions, the complex also displays intense bands at 485 and 435 nm due to metal-to-bridging ligand charge transfer (MLCT), and these bands arise because of the transitions from the molecular orbitals 166 → 168, 167 → 168, 163 → 169, 164 → 169, 165 → 169, and 167 → 169, respectively. This can be explained on the basis of the fact that the π-π^* transitions of the bridged ligand are lower in energy than those of bpy. In addition to these bands, theoretically, an additional intense band is observed at 412 nm and come up because of the transitions from 163 → 168 and 163 → 169. Although, the nature of transitions is comparable with the experimentally observed results, the wavelengths of absorption corresponding to these transitions in gas phase are slightly different from the actual absorptions. These transitions are responsible for the explanations of many properties including colour, sensing capabilities, binding capacity, and many more. These different types of charge transfers can be visualized using MO diagrams, provided in Figures 2(a) to 2(q) with the molecular orbital number given in the parenthesis and the nature of transitions in Table 2, respectively.

One of the important aspects of this work is to study the effect of solvents on the excitation energies. We adopt two-step approach to study the effect of solvent on excitation energies. In the first step we calculate excitation energies in two different solvents, namely, CH_3CN and DMSO, on gas phase optimized structure. We further go on calculating excitation energies on solvent phase optimized geometry in

Table 1: (a) Comparison of selected bond lengths and (b) comparison of selected bond angles.

(a)

Serial number	Name of bond lengths	Bond lengths	
		Computed	Experimental
1	Ru-N6	2.060	2.033
2	Ru-N4	2.072	2.039
3	Ru-N3	2.067	2.039
4	Ru-N5	2.074	2.074
5	Ru-N8	2.112	2.077
6	Ru-N1	2.093	2.093

(b)

Serial number	Name of bond angles	Bond angles (in degree)	
		Computed	Experimental
1	N6-Ru-N4	89.84	89.20
2	N6-Ru-N3	97.06	96.47
3	N6-Ru-N5	78.44	78.88
4	N4-Ru-N3	78.44	79.21
5	N4-Ru-N5	98.45	100.60
6	N3-Ru-N5	174.61	175.35
7	N6-Ru-N8	173.26	172.98
8	N4-Ru-N8	95.45	95.51
9	N3-Ru-N8	88.08	89.54
10	N5-Ru-N8	96.63	95.10
11	N6-Ru-N1	97.23	97.48
12	N4-Ru-N1	171.38	170.99
13	N3-Ru-N1	95.75	93.97
14	N5-Ru-N1	87.80	86.67
15	N8-Ru-N1	77.85	78.42

the second step. On the basis of calculated results reported in Table 3, it is found that there is small increase in the values of excitation energies in case of CH_3CN and DMSO in comparison to the excitation energies of gas phase geometry. The maximum shift in excitation energies obtained in case of CH_3CN and DMSO is 0.1201 and 0.1180 eV, respectively, from the gas phase excitation energies values, amongst the first ten excitations. On the other hand the maximum shift obtained in the excitation energy values between gas and solvent phase optimized geometries for the same solvent (CH_3CN) is 0.0315 eV. The difference between excitation energies of gas phase and solvent phase optimized geometry is very small and is almost in the range of gas phase optimized excitation energy values. However, small alterations in the values of excitation energies could be attributed to the interaction of fields produced by ligands and metal atom with the field of solvent molecules which affect the energy gap between the various molecular orbitals and lead to the shift in the values of excitation energies. Since the strength of these interactions varies from solvent to solvent, this leads to the shift in excitation energies accordingly. One of the main components for such interactions is the strength of hydrogen bonding, which is different for different solvents. These shifts are almost equal in magnitude because of similar dipole moments for both of these solvents. However, slight variation may be due to different hydrogen bonding capacities and different arrangement of atoms in the space, which are responsible for the production of field interactions. These solvent interactions will lead to the increase in the electron density at the metal center resulting in decrease of the band energies which leads to shift in the values of excitation energies.

From the above discussion it may also be concluded that there are two main factors responsible for the change in energy gap of various molecular orbitals which are polarity and hydrogen bonding ability of the solvent. Due to difference in energy gap, the complex absorbs at different wavelengths and displays different colour in different solvents. This conclusion is reflected from the experimental observations that the complex changes its colour from yellow-orange in CH_3CN to orange-brown in DMSO.

4. Conclusions

The recognition and sensing of anions has emerged recently as a key research area within the generalized area of

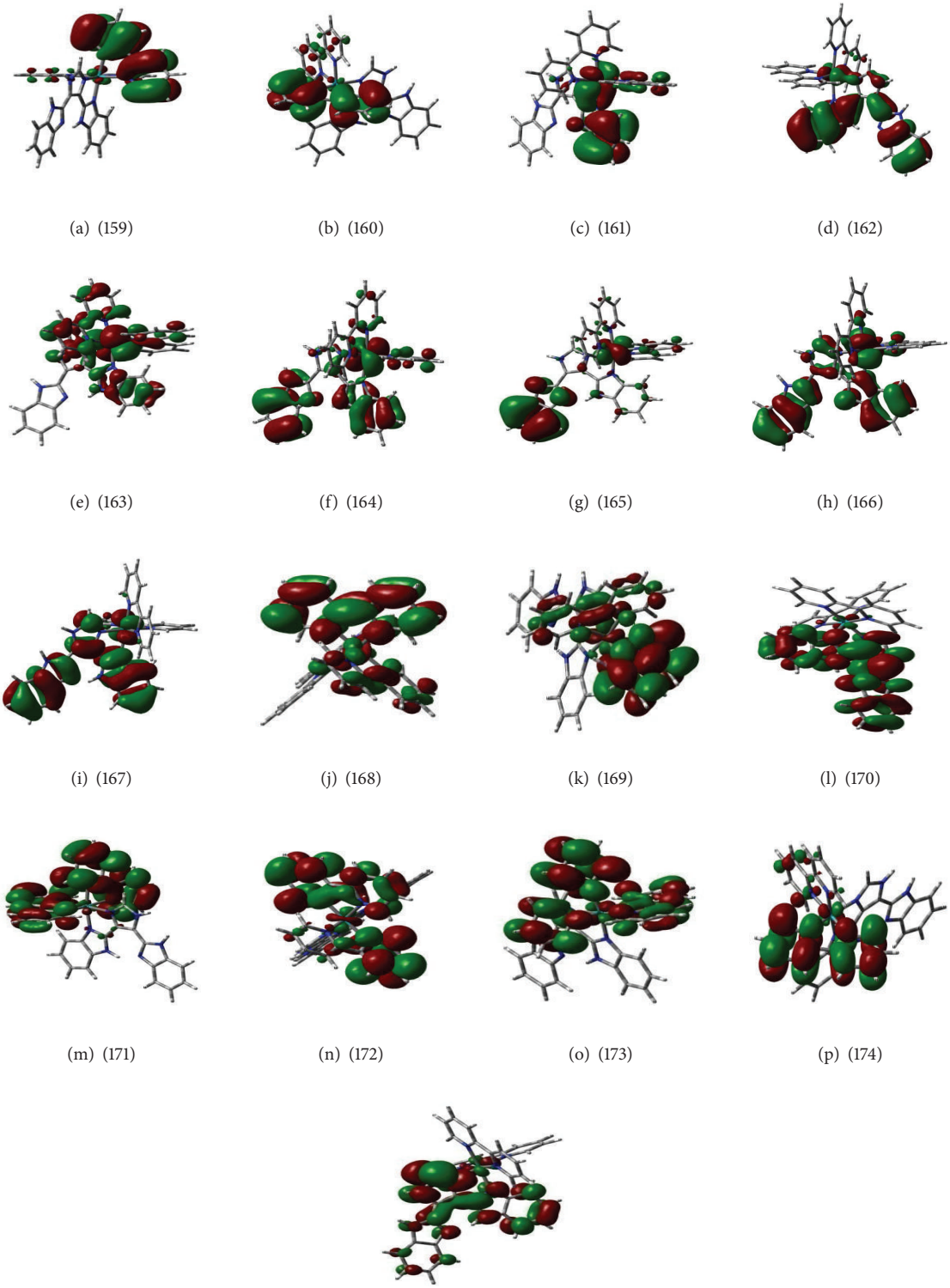

(a) (159) (b) (160) (c) (161) (d) (162)

(e) (163) (f) (164) (g) (165) (h) (166)

(i) (167) (j) (168) (k) (169) (l) (170)

(m) (171) (n) (172) (o) (173) (p) (174)

(q) (175)

Figure 2

Table 2: Electronic transitions computed at the level of time-dependent density functional theory for $[(bpy)_2Ru(H_3Imbzim)]^{+2}$ complex.

Electronic states	Excitation energy (eV)	Wavelength (nm)	Oscillator strength	Types of transition	Nature of transition	Assignment
01	2.5529	485.67	0.2010	166 → 168	−0.41477	MLCT
				167 → 168	0.47766	MLCT
02	2.8490	435.19	0.1570	163 → 169	−0.28104	MLCT
				164 → 169	0.34023	MLCT
				165 → 169	−0.29161	Mixed
				167 → 169	0.30828	LL
03	3.0068	412.35	0.0807	163 → 168	0.54778	MLCT
				163 → 169	0.28194	MLCT
04	3.2830	377.66	0.1804	166 → 170	−0.30132	MLCT
				167 → 170	0.51815	MLCT
05	3.4396	360.46	0.2244	164 → 170	0.35197	MLCT
				165 → 170	−0.26725	MLCT
				166 → 170	0.42918	MLCT
				167 → 170	0.25544	LL
06	3.5832	346.01	0.1440	163 → 170	−0.26963	MLCT
				164 → 170	−0.28653	MLCT
				165 → 170	0.31145	MLCT
				166 → 170	0.36692	MLCT
07	4.3353	286	0.0648	161 → 170	0.43704	LL
				162 → 168	0.12355	LL
				162 → 169	0.21078	LL
				162 → 170	0.32326	LL
				165 → 172	0.13110	LL
				165 → 173	−0.13259	LL
				166 → 173	−0.10353	LL
				167 → 175	−0.12937	LL
08	5.2682	235	0.0226	159 → 171	−0.16029	LL
				159 → 172	−0.11813	LL
				160 → 171	0.39092	LL
				161 → 172	−0.18365	LL
				161 → 173	0.20017	LL
				161 → 174	0.25480	LL
				162 → 173	0.12910	LL
				162 → 174	0.10284	LL
				163 → 173	−0.12647	LL
				163 → 174	−0.12578	LL

supramolecular chemistry for the important role played by anions in biological, industrial, and environmental processes [1–8]. In this study, optimization was carried at DFT level, while electronic absorption spectra were computed as vertical electronic excitations from the ground state using TD-DFT approach. We have chosen PBE1 hybrid functional for the calculation of ground state and excited state properties and the effect of solvent on excitation energies was taken carefully by using polarizable continuum model [26] (PCM). The comparison of optimized geometry with X-ray geometry, effect of CH_3CH and DMSO on the excitation energies, comparison of absorption spectra, and the assignment of nature of different charge transfers have been done in the present work.

Finally, it is observed that DFT and TD-DFT calculations performed on this complex are adequate in the reproduction of excitation and absorption energies and thus can be used in the design of anion sensors. Based on good reliability of

Table 3: Effect of solventson excitation energies.

Electronic state	Excitation energy in gas phase (eV)	Excitation energy in DMSO (eV)	Excitation energy in CH_3CN (eV)	*Excitation energy in CH_3CN (eV)
1	2.5529	2.6503	2.6486	2.6485
2	2.6545	2.6702	2.6682	2.6711
3	2.7310	2.7901	2.7887	2.7849
4	2.8490	2.8370	2.8356	2.8239
5	3.0068	2.9916	2.9943	2.9758
6	3.0859	3.1035	3.1070	3.0976
7	3.1545	3.1715	3.1719	3.1631
8	3.2052	3.2905	3.2937	3.2835
9	3.2830	3.4015	3.4031	3.3822
10	3.4396	3.5296	3.5283	3.4968

*Excitation energy values obtained from solvent phase optimized geometry.

DFT and TD-DFT methods, future research studies should consider this method of calculating ground and excited state properties.

Conflict of Interests

The authors declare that there is no conflict of interests regarding the publication of this paper.

Acknowledgment

The authors would like to thank Central University of Gujarat, Gandhinagar, for providing basic computational facility.

References

[1] J. L. Sessler, P. A. Gale, and W. S. Cho, *Anion Receptor Chemistry*, Royal Society of Chemistry, Cambridge, UK, 2006.

[2] R. Martinez-Manez and F. Sancenon, "Fluorogenic and chromogenic chemosensors and reagents for anions," *Chemical Reviews*, vol. 103, pp. 4419–4476, 2003.

[3] A. Bianchi, K. Bowman-James, and E. Garcia-Espana, *Supramolecular Chemistry of Anions*, Wiley-VCH, New York, NY, USA, 1997.

[4] J. M. Lehn, *Supramolecular Chemistry Concepts and Perspective*, Wiley-VCH, Weinheim, Germany, 1995.

[5] V. Amendola, D. Esteban-Gómez, L. Fabbrizzi, and M. Licchelli, "What anions do to N-H-containing receptors," *Accounts of Chemical Research*, vol. 39, no. 5, pp. 343–353, 2006.

[6] C. Suksai and T. Tuntulani, "Chromogenic anion sensors," *Topics in Current Chemistry*, vol. 255, pp. 163–198, 2005.

[7] J. Pérez and L. Riera, "Stable metal-organic complexes as anion hosts," *Chemical Society Reviews*, vol. 37, no. 12, pp. 2658–2667, 2008.

[8] S.-T. Lam, N. Zhu, and V. W.-W. Yam, "Synthesis and characterization of luminescent rhenium(l) tricarbonyl diimine complexes with a triarylboron moiety and the study of their fluoride ion-binding properties," *Inorganic Chemistry*, vol. 48, no. 20, pp. 9664–9670, 2009.

[9] K. L. Kirk, *Biochemistry of the Halogens and Inorganic Halides*, Plenum Press, New York, NY, USA, 1991.

[10] R. L. P. Adams, J. T. Knowler, and D. P. Leader, *The Biochemistry of the Nucleic Acids*, Chapman & Hall, New York, NY, USA, 10th edition, 1986.

[11] N. Kartner, J. W. Hanrahan, T. J. Jensen et al., "Expression of the cystic fibrosis gene in non-epithelial invertebrate cells produces a regulated anion conductance," *Cell*, vol. 64, no. 4, pp. 681–691, 1991.

[12] K. Renkawek and G. J. C. G. M. Bosman, "Anion exchange proteins are a component of corpora amylacea in Alzheimer disease brain," *NeuroReport*, vol. 6, no. 6, pp. 929–932, 1995.

[13] B. Moss, "A land awash with nutrients—the problem of eutrophication," *Chemistry and Industry*, pp. 407–411, 1996.

[14] C. Glidewell, "Nitrate/nitrite controversy," *Chemistry in Britain*, vol. 26, no. 2, pp. 137–140, 1990.

[15] S. Ayoob and A. K. Gupta, "Fluoride in drinking water: a review on the status and stress effects," *Critical Reviews in Environmental Science and Technology*, vol. 36, no. 6, pp. 433–487, 2006.

[16] M. Kleerekoper, "The role of fluoride in the prevention of osteoporosis," *Endocrinology and Metabolism Clinics of North America*, vol. 27, no. 2, pp. 441–452, 1998.

[17] P. Anzebacher, D. S. Tyson, K. Jurslkova, and F. N. Castellano, "Luminescence lifetime-based sensor for cyanide and related anions," *Journal of the American Chemical Society*, vol. 124, pp. 6232–6233, 2002.

[18] T. Mizuno, W.-H. Wei, L. R. Eller, and J. L. Sessler, "Phenanthroline complexes bearing fused dipyrrolylquinoxaline anion recognition sites: efficient fluoride anion receptors," *Journal of the American Chemical Society*, vol. 124, no. 7, pp. 1134–1135, 2002.

[19] P. D. Beer, F. Szemes, V. Balzani et al., "Anion selective recognition and sensing by novel macrocyclic transition metal receptor systems. 1H NMR, electrochemical, and photophysical investigations," *Journal of the American Chemical Society*, vol. 119, pp. 11864–11875, 1997.

[20] Y. Cui, H.-J. Mo, J.-C. Chen et al., "Anion-selective interaction and colorimeter by an optical metalloreceptor based on ruthenium(II) 2,2′-biimidazole: hydrogen bonding and proton transfer," *Inorganic Chemistry*, vol. 46, no. 16, pp. 6427–6436, 2007.

[21] S. Debasish, D. Shyamal, B. Chanchal, D. Supriya, and B. Sujoy, "Monometallic and bimetallic ruthenium(II) complexes

derived from 4,5-Bis(benzimidazol-2-yl)imidazole (H3Imbzim) and 2,2′-bipyridine as colorimetric sensors for anions: synthesis, characterization, and binding studies," *Inorganic Chemistry*, vol. 49, pp. 2334–2348, 2010.

[22] M. J. Frisch, G. W. Trucks, H. B. Schlegel et al., *Gaussian 03 Revision B 05 Pople*, Gaussian, Pittsburgh, Pa, USA, 2003.

[23] V. Barone and M. Cossi, "Quantum calculation of molecular energies and energy gradients in solution by a conductor solvent model," *Journal of Physical Chemistry A*, vol. 102, no. 11, pp. 1995–2001, 1998.

[24] P. J. Hay and W. R. Wadt, "Ab initio effective core potentials for molecular calculations. Potentials for main group elements Na to Bi," *The Journal of Chemical Physics*, vol. 82, no. 1, pp. 284–298, 1985.

[25] C. Adamo and V. Barone, "Toward reliable density functional methods without adjustable parameters: the PBE0 model," *Journal of Chemical Physics*, vol. 110, no. 13, pp. 6158–6170, 1999.

[26] C. Adamo and V. Barone, "Toward reliable adiabatic connection models free from adjustable parameters," *Chemical Physics Letters*, vol. 274, pp. 242–250, 1997.

[27] C. Adamo and V. Barone, "Exchange functionals with improved long-range behavior and adiabatic connection methods without adjustable parameters: the mPW and mPW1PW models," *Journal of Chemical Physics*, vol. 108, no. 2, pp. 664–675, 1998.

[28] C. Adamo and D. Jacquemin, "The calculations of excited-state properties with time-dependent density functional theory," *Chemical Society Reviews*, vol. 42, pp. 845–856, 2013.

[29] J. Tomasi, B. Mennucci, and R. Cammi, "Quantum mechanical continuum solvation models," *Chemical Reviews*, vol. 105, no. 8, pp. 2999–3093, 2005.